

Electron microscopy of silicon monophosphide precipitates in P-diffused silicon

M. SERVIDORI, A. ARMIGLIATO

Laboratorio LAMEL-CNR, Via de' Castagnoli 1, Bologna, Italy

Precipitates of a second phase in P-diffused (111) and (110) silicon wafers were revealed by X-ray topography and studied by transmission electron microscopy. The structural data derived from the analysis of the images and the corresponding diffraction patterns resulted in agreement with the ones recently reported by Wadsten, in his X-ray study on synthetic SiP single crystals. Therefore the precipitates were assigned a SiP base-centred orthorhombic structure with $a = 3.51 \text{ \AA}$, $b = 20.59 \text{ \AA}$ and $c = 13.60 \text{ \AA}$.

The sign of the calculated values of the misfit parameters between the two phases and the morphology of the precipitates were related to the tensile stress induced by the phosphorus diffusion into silicon.

1. Introduction

In a recent paper [1] a detailed X-ray study of the heterogeneous nucleation and the growth of dislocation lines associated to precipitates due to thermal diffusion of phosphorus into silicon was reported. The presence of this second phase confirmed the hypothesis that the difference between the total amount of dopant, introduced into the silicon lattice by the diffusion process, and its electrically active fraction, was due, at least in part, to precipitation phenomena [1, 2].

From the images of the precipitates taken by X-ray topography no structural information can be derived, because of the precipitate size. Therefore a study of the crystallography of the observed particles was undertaken with the electron microscope, because the structural results published by other authors [3-5] on precipitates in P-diffused silicon are incomplete and do not lead to an unequivocal set of crystallographic parameters.

The experimental work reported here is a part of a systematic investigation on the parameters controlling the predeposition process of phosphorus, as well as on the presently incomplete Si-P phase diagram available in the literature [6].

Some results on the kinetics of P-predeposition have been reported in a separate paper [2].

306



Figure 1 $\bar{2}20$ X-ray topograph showing precipitates in P-diffused (111) silicon. $\text{CuK}\alpha_1$ radiation.

2. Experimental procedures

The specimens we have observed were p-type

Czochralski grown silicon slices both of (111) and (110) orientations. The predeposition process for P impurities was performed at 1000°C for 12, 25 and 50 min in a 94% N₂ and 6% O₂ atmosphere, with POCl₃ as the source. The X-ray images taken on the slices diffused for 25 min and 50 min have been reported in the above cited paper [1]; the one corresponding to a diffusion time of 12 min is shown in Fig. 1. The precipitates displayed in this figure exhibit the same morphology as the ones in [1], but are not associated to straight dislocations.

From these slices we obtained specimens suitable for the electron microscope by means of the chemical jet-etching technique [7]. The instrument used was a Siemens Elmiskop 101, working at 100 kV; with such an accelerating voltage it is possible to observe layers of silicon several thousands of Angstroms thick. Therefore, since it was demonstrated [1] that the observed precipitates mostly lie just within this depth, care was taken during the thinning procedure in preserving the diffused surface. As in many structural studies a wide range of operating reflections is often required, a $\pm 45^\circ$ double tilting cartridge was used in our experiments.

3. Results and discussion

3.1. Precipitates in (111) wafers

The electron micrographs taken on (111) specimens revealed that the dots in the topograph shown in Fig. 1 consisted of aggregates of flat rod-like precipitates. A typical image of such a morphology is reported in Fig. 2. These particles

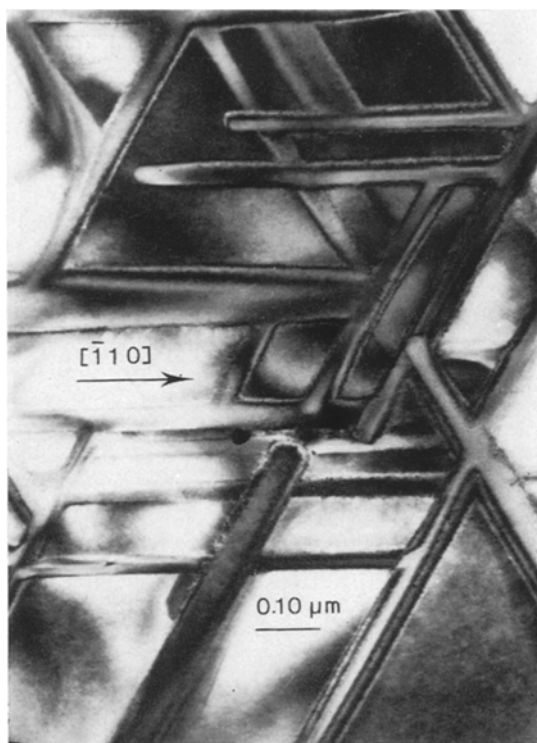


Figure 2 Electron micrograph of an aggregate of flat rod-like precipitates.

were found to be aligned with the $\langle 110 \rangle$ directions of silicon parallel to the foil surface and to lie on the inclined $\{111\}$ planes, as was confirmed by stereo pairs. Other authors [3-5] observed similar precipitates in P-doped silicon

TABLE I

Authors	Technique	Formula and structure	Space group	Lattice parameters	Orientation relationships
Schmidt and Stickler (1964)	Electron diffraction	SiP Orthorhombic	—	$a = 6.90 \text{ \AA}$ $b = 9.40 \text{ \AA}$ $c = 7.68 \text{ \AA}$	$[111]_{\text{Si}} \parallel [010]_{\text{SiP}}$ $[110]_{\text{Si}} \parallel [001]_{\text{SiP}}$
Beck and Stickler (1966)	Electron and X-ray diffraction	SiP Orthorhombic	—	$a = 6.80 \text{ \AA}$ $b = 10.25 \text{ \AA}$ $c = 8.25 \text{ \AA}$	$(110)_{\text{Si}} \parallel (102)_{\text{SiP}}$ $[1\bar{1}1]_{\text{Si}} \parallel [0\bar{1}0]_{\text{SiP}}$ $[\bar{1}10]_{\text{Si}} \parallel [241]_{\text{SiP}}$
Levine, Washburn and Thomas (1967)	Electron diffraction	No formula Probably C-orthorhombic	—	$a = 6.3 \text{ \AA}$ $b = 3.8 \text{ \AA}$ $c = 6.75 \text{ \AA}$	$[\bar{1}10]_{\text{Si}} \parallel [010]_{\text{P}}$ $[11\bar{1}]_{\text{Si}} \parallel [001]_{\text{P}}$ (P = precipitate)
Wadsten (1973)	X-ray diffraction	SiP C-orthorhombic	$Cmc2_1$ (No. 36)	$a = 3.510 \pm 0.001 \text{ \AA}$ $b = 20.592 \pm 0.006 \text{ \AA}$ $c = 13.601 \pm 0.004 \text{ \AA}$	—

and deduced some structural information about them from electron diffraction patterns; mostly, they suggested for these particles an orthorhombic structure and a SiP formula. In addition, Wadsten [8] has very recently determined the structure of SiP single crystals using X-ray diffraction techniques. All these data are summarized in Table I. It is worthwhile to notice that there is a large scattering among the structural parameters of precipitates in P-doped silicon and, in particular, that none of them agrees with the ones of synthetic single crystals.

The selected-area diffraction (SAD) patterns we used for our structural determinations were taken on single flat rods, like the one in Fig. 3. The corresponding SAD patterns exhibited the presence of extra spots in addition to the ones of the silicon matrix. At least within the degree of accuracy attainable in electron microscopy, the experimental d -values, obtained from these extra spots, were found to be in quite good agreement with the ones calculated from the

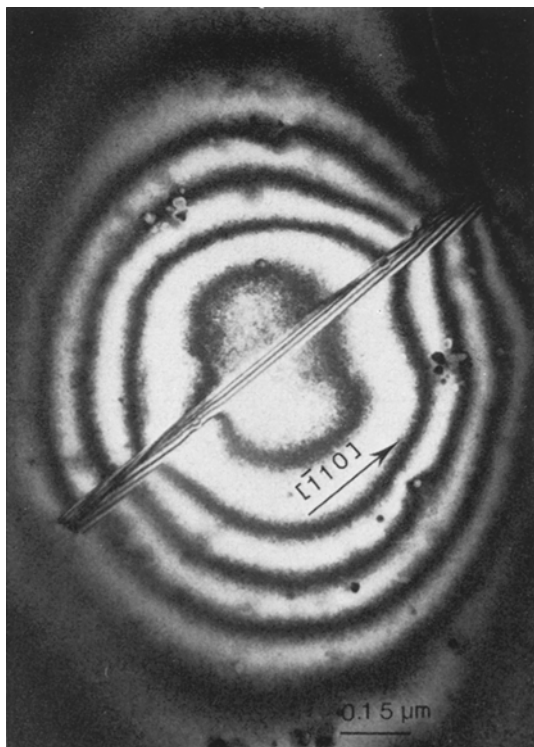


Figure 3 Electron micrograph of a single precipitate surrounded by thickness fringes, which are due to preferential attack during the chemical thinning of the specimen.

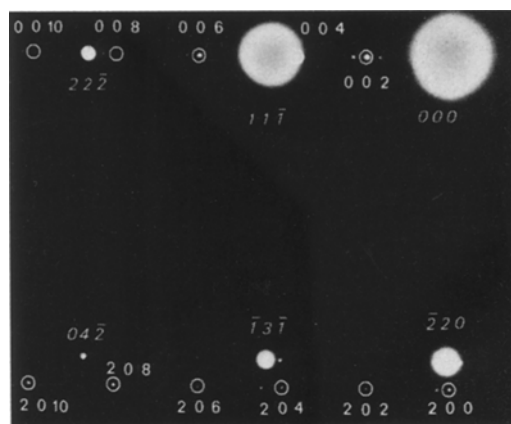


Figure 4 Selected-area diffraction (SAD) pattern of the precipitate in Fig. 3, taken in the (112) projection. The encircled spots were used for d -values determination; the other ones arise from double diffraction. The Miller indices in italics refer to the matrix spots.

lattice parameters of the base-centred orthorhombic structure given by Wadsten [8]. These figures are reported in Table II.

TABLE II

hkl	d (Å)		hkl	d (Å)	
	Wadsten	This work		Wadsten	This work
002	6.80 ₀	6.78	224	1.54 ₂	1.52
023	4.14 ₉	4.12	206	1.38 ₈	1.39
004	3.40 ₀	3.39	069	1.38 ₃	1.37
024	3.22 ₉	3.27	0010	1.36 ₀	1.36
112	3.08 ₄	3.07	246	1.34 ₀	1.32
006	2.26 ₇	2.26	208	1.22 ₁	1.21
046	2.07 ₄	2.06	248	1.18 ₈	1.17
200	1.75 ₅	1.76	2010	1.07 ₅	1.08
008	1.70 ₀	1.70	390	1.04 ₂	1.04
202	1.69 ₉	1.70	392	1.03 ₀	1.03
223	1.61 ₆	1.60	394	0.99 ₆	0.99
048	1.61 ₄	1.60	396	0.94 ₇	0.94
204	1.56 ₀	1.56	400	0.87 ₈	0.88

Since the particle in Fig. 3 was aligned with the $[\bar{1}10]$ direction and on the $(11\bar{1})$ plane of the silicon, it was concluded that a diffraction pattern corresponding to the (112) projection would display spots suitable for deducing the orientation relationships between the two phases. In fact from the pattern reported in Fig. 4 we deduced the following relationships:

$$\begin{aligned} [100]_{\text{SiP}} & \parallel [\bar{1}10]_{\text{Si}} \\ [001]_{\text{SiP}} & \parallel [11\bar{1}]_{\text{Si}} \end{aligned}$$

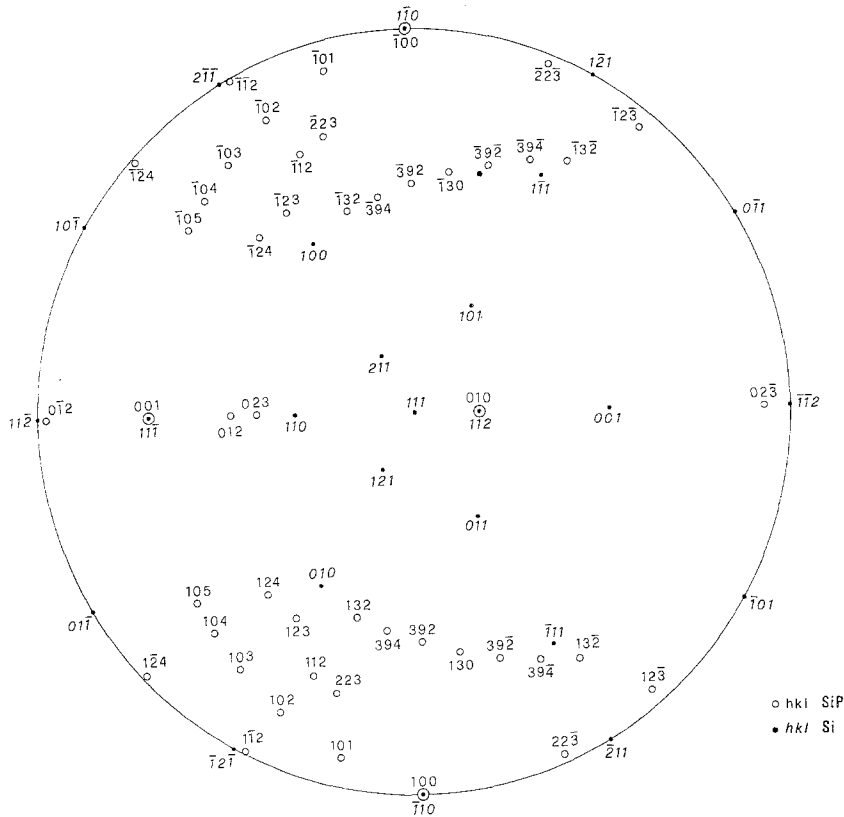


Figure 5 (111) stereographic projection of silicon representing the crystallographic orientation relationships between SiP and Si.

and consequently

$$[010]_{SiP} \parallel [112]_{Si}.$$

These conditions allowed us to draw in the (111) stereographic projection of silicon the poles of the SiP planes (Fig. 5).

The electron diffraction of Fig. 6, corresponding to a specimen tilt of about 1.5° around the $[\bar{1}10]$ direction of silicon, reveals the spots from the $(0\bar{1}2)$, $(\bar{1}\bar{1}2)$, $(\bar{1}\bar{2}4)$ planes of SiP, in agreement with the stereographic projection.

The observed precipitates were about 1 μm long, but only about 200 Å thick. This explains the appearance of streaking effects in some diffraction pattern.

In all the SAD we examined, no reflection violating the limiting conditions of the $Cmc2_1$ space group was observed. Double diffraction effects occurred only between the lattice planes of silicon and of silicon monophosphide.

The orientation relationships as well as the lattice parameters of SiP were confirmed by the

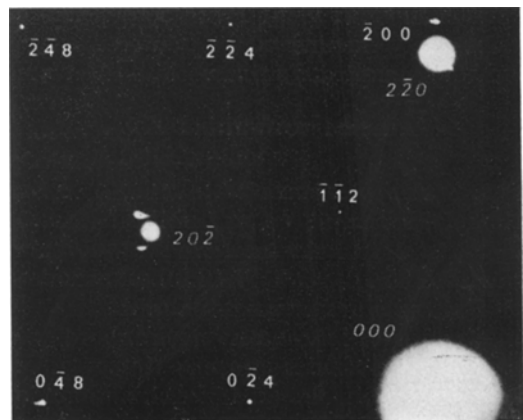


Figure 6 SAD pattern taken after a specimen tilt of about 1.5° around the $[\bar{1}10]$ direction.

spacing of the Moiré fringes which appeared on the images of the precipitates. Moiré spacings of 21 and 40 Å were measured in the pictures of Fig. 7a and b, which were taken in two-beam

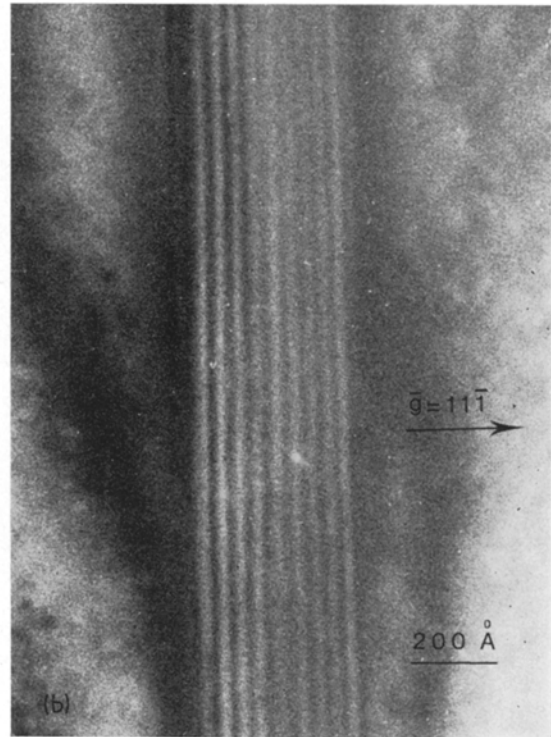
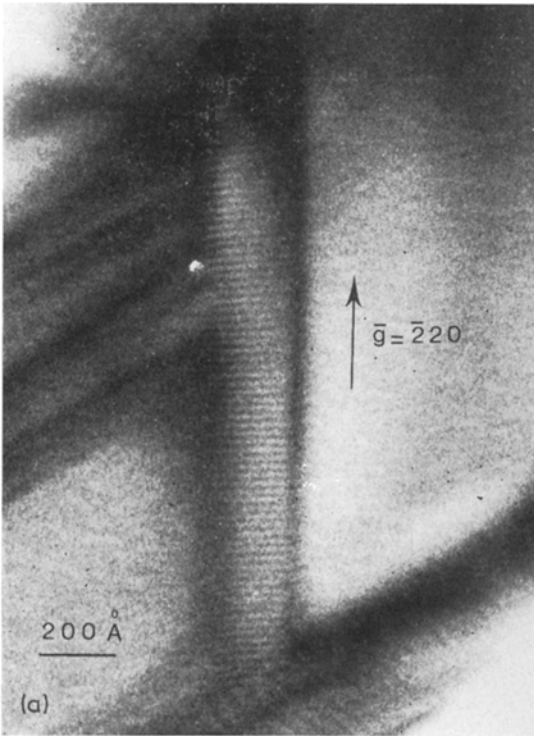
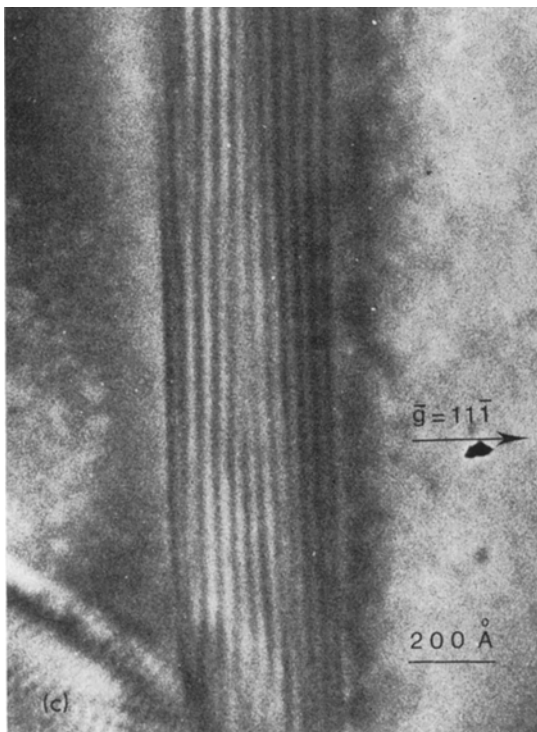


Figure 7 Parallel Moiré fringes in SiP precipitates with spacings of 21 Å (a) and 40 Å (b). Dislocations imaged by the 40 Å fringes, like the one in (c), were sometimes observed.



conditions with $\bar{2}20$ and $11\bar{1}$ operating reflections, respectively.

The planes which give rise to these observed fringes are the couples $(\bar{2}20)_{\text{Si}} - (200)_{\text{SiP}}$ and $(11\bar{1})_{\text{Si}} - (004)_{\text{SiP}}$; from the corresponding d -values we get 20.4 and 40.3 Å as expected Moiré spacings, for fringes perpendicular and parallel to the particles, respectively. The agreement between the experimental and the calculated figures was good, although a fluctuation in the 40 Å spacing was sometimes observed, owing to the presence of dislocation lines (Fig. 7c) and/or to elastic strains. The greater sensitivity of the 40 Å spacing to these strains can be explained according to the fact that the smaller the particle size in a given direction, the larger the elastic strain required to accommodate the mismatch.

3.2. Precipitates in (110) wafers

Precipitates of the same flat rod-like shape as in the previous case were also observed in these slices. The particles were found to lie along two

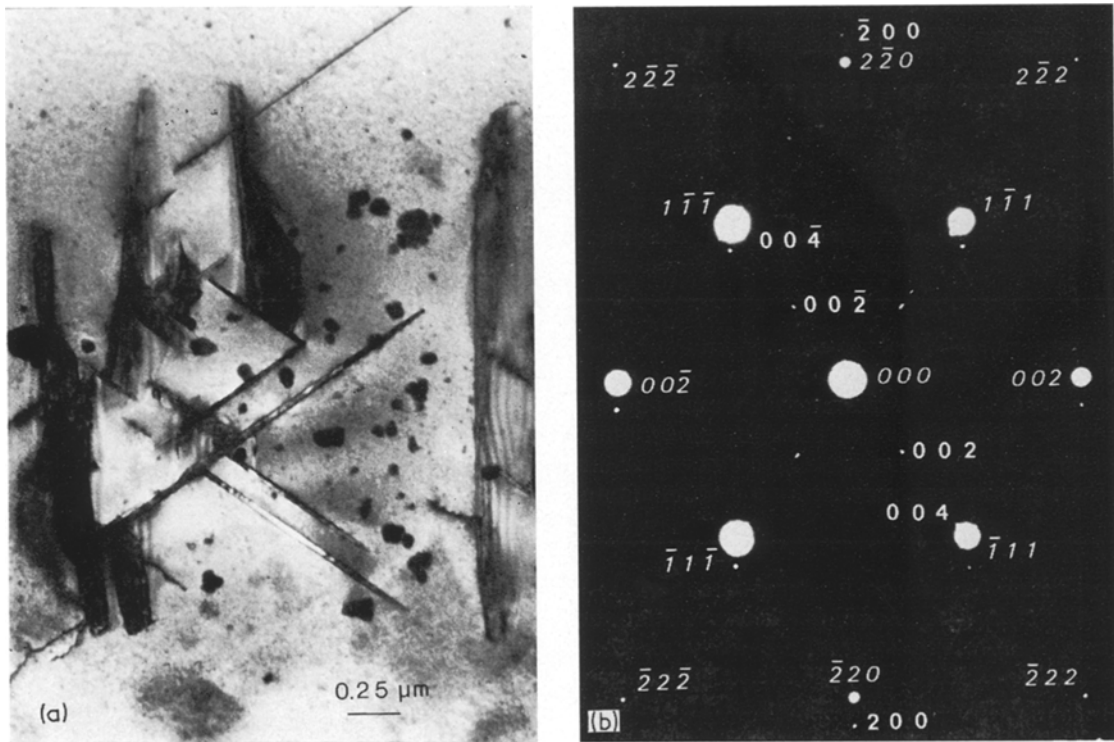


Figure 8 Electron micrograph (a) and corresponding SAD pattern (b) of SiP precipitates in a (110) silicon wafer. The Miller indices in italics refer to the matrix spots.

different directions, namely the $\langle 112 \rangle$ and the $[\bar{1}10]$ directions parallel to the foil. These directions are the traces of the $\{111\}$ planes perpendicular to the specimen surface and of the inclined (111) or $(11\bar{1})$ planes, respectively.

In Fig. 8 an aggregate of such precipitates is shown, together with the corresponding SAD pattern. From an inspection of Fig. 8 it was deduced that, even for this orientation of the slices, the structure of the precipitates as well as their dimensions were the same as the ones found before. The structural information so obtained enabled us to determine the orientation relationships between the two phases.

Fig. 9 represents the (110) stereographic projection of silicon which includes the poles of the SiP planes. In this case the orientation relationships are the following ones:

- (1) $[100]_{\text{SiP}} \parallel [\bar{1}10]_{\text{Si}}$ (2) $[100]_{\text{SiP}} \parallel [110]_{\text{Si}}$
- $[001]_{\text{SiP}} \parallel [11\bar{1}]_{\text{Si}}$ $[001]_{\text{SiP}} \parallel [\bar{1}11]_{\text{Si}}$
- $[010]_{\text{SiP}} \parallel [112]_{\text{Si}}$ $[010]_{\text{SiP}} \parallel [\bar{1}1\bar{2}]_{\text{Si}}$

The others have been omitted as equivalent.

3.3. Misfit between SiP and Si lattices

From the values of the interplanar spacings of the matrix and of the precipitates, we obtained for the misfit parameters $\delta_c = +0.084$ in the $\langle 1\bar{1}1 \rangle$ directions of silicon (c -axis of SiP) and $\delta_a = -0.086$ in the $\langle \bar{1}10 \rangle$ directions (a -axis of SiP). Here we have assumed that δ is positive when the spacing of the particle planes is larger than the one of the corresponding parallel planes of the matrix.

Since the precipitates nucleate and grow with their c -axis perpendicular to the more extended interface between the two phases, we conclude that they play an important role in relieving the tensile stress, which is known to develop during the P-predeposition.

As in the matrix around the particles a compressive stress predominates, the X-ray image, due to the precipitates which are near the X-ray exit surface, should exhibit a black and white contrast (the so-called Friedel contrast [9]) with its black side on the side of positive g . This is just what appears in Fig. 1.

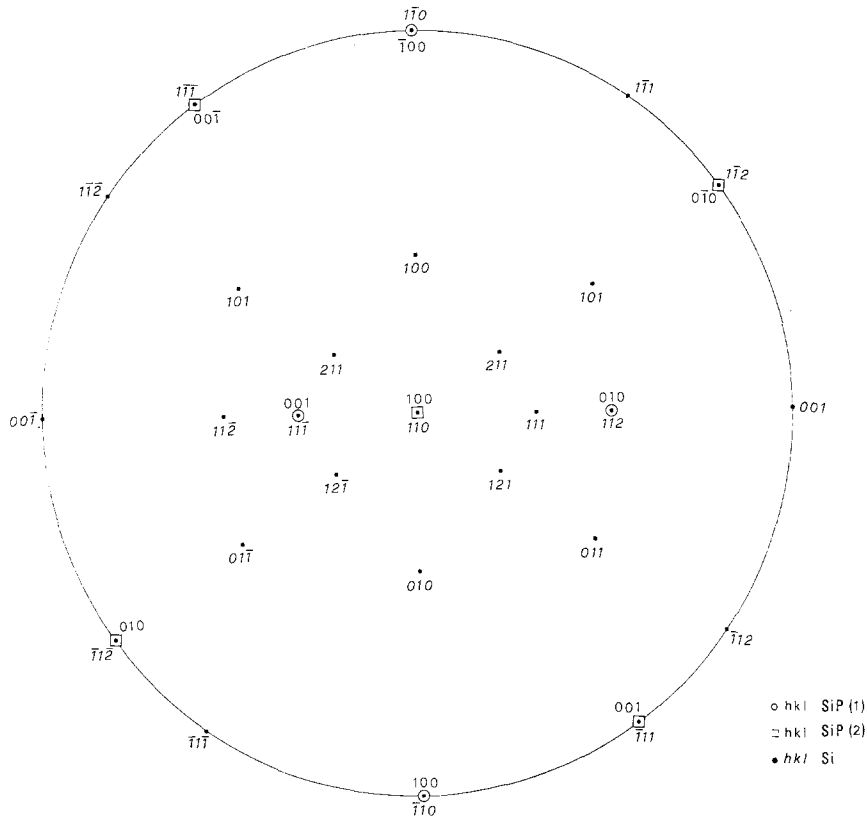


Figure 9 (110) stereographic projection of silicon representing the crystallographic orientation relationships between SiP and Si. SiP (1) and SiP (2) refer to inclined and perpendicular precipitates, respectively.

4. Conclusions

X-ray topographic observations carried out in P-diffused (111) silicon wafers at 1000°C for 12 min revealed the presence of precipitates of a second phase, very similar to the ones reported in a previous paper [1]. The insufficient resolution limit of this technique did not allow us to obtain structural information about these particles; transmission electron microscopy was therefore employed on (111) and (110) specimens subjected to the same diffusion process. Each dot-like precipitate observed in X-ray topographs was found to consist of aggregates of flat rods lying on the $\{\bar{1}11\}$ planes of the silicon foil. From SAD patterns taken on these precipitates, it was possible to obtain the interplanar d -spacings as well as the orientation relationships between the particles and the matrix. From a comparison with the structural parameters reported by Wadsten [8], who performed the most accurate structure determination presently available in literature, we deduced

that the precipitates were SiP single crystals and fitted the base-centred orthorhombic structure with space group $Cmc2_1$. Therefore, the cell parameters of the precipitates were $a = 3.51\text{Å}$, $b = 20.59\text{Å}$ and $c = 13.60\text{Å}$. The agreement was confirmed by the absence in the diffraction patterns of precipitate reflections forbidden by the space group $Cmc2_1$, and by the appearance in the electron micrographs of parallel Moiré fringes with spacings quite close to the computed ones.

Prussin [10] calculated the stresses inside an infinite lamella which is subjected to a diffusion process. A feature of his calculation is that the stress is purely tensile for phosphorus diffusion and acts parallel to the surface of the lamella. Since along the c -axis of SiP a positive misfit ($\delta_c = +0.084$) develops, the precipitates play an important role in relieving the diffusion induced tensile stress. In (111) wafers, because of the 70.5° inclination of the $\{\bar{1}11\}$ planes, the component of the misfit in the plane of diffusion

is large; in (110) wafers, for the precipitates perpendicular to the foil, this component has its maximum value, whereas for the inclined precipitates it is smaller. Therefore the growth of the flat rod particles perpendicular to the specimen surface seems to be energetically favoured. At present experiments are in progress in order to confirm the validity of this assumption.

Acknowledgements

We are indebted to Mr P. Negrini and Mr I. Vecchi for their technical assistance in the specimen preparation. Mr L. Dori and Mr A. Zani are also gratefully acknowledged.

References

1. C. GHEZZI and M. SERVIDORI, *J. Mater. Sci.* **9** (1974) 1797.
2. P. NEGRINI, D. NOBILI and S. SOLMI, to be published.
3. P. F. SCHMIDT and R. STICKLER, *J. Electrochem. Soc.* **111** (1964) 1188.
4. C. G. BECK and R. STICKLER, *J. Appl. Phys.* **37** (1966) 4683.
5. E. LEVINE, J. WASHBURN and G. THOMAS, *J. Appl. Phys.* **38** (1967) 87.
6. V. M. GLAZOV and V. S. ZEMSKOV, "Physico-Chemical Principles of Semiconductor Doping" (JPST Press, Cap. No 2205, Jerusalem 1968) p. 141.
7. P. G. MERLI and U. VALDRÉ, *J. Phys. E: Sci. Instrum.* **5** (1972) 933.
8. T. WADSTEN, *Univ. Stockholm Chem. Communic.* No 7, (1973) 1.
9. G. H. SCHWUTTKE and J. K. HOWARD, *J. Appl. Phys.* **39** (1968) 1581.
10. S. PRUSSIN, *J. Appl. Phys.* **32** (1961) 1876.

Received 29 July and accepted 28 August 1974.